

# The impact of imagistic evaluation of premalignant and malignant lesions of the breast confirmed in histopathological terms

ALINA OANA RUSU-MOLDOVAN<sup>1)</sup>, MĂDĂLINA GABRIELA RADU<sup>2)</sup>, MARIA IULIANA GRUIA<sup>3)</sup>,  
 DAN NICOLAE PĂTROI<sup>4)</sup>, CAMELIA MANUELA MÎRZA<sup>5)</sup>, DAN MIHU<sup>6)</sup>

<sup>1)</sup>Department of Surgery III, "Prof. Dr. Alexandru Trestioreanu" Institute of Oncology, Bucharest, Romania

<sup>2)</sup>Department of Pathology, "Prof. Dr. Alexandru Trestioreanu" Institute of Oncology, Bucharest, Romania

<sup>3)</sup>Department of Biochemistry and Radiobiology, "Prof. Dr. Alexandru Trestioreanu" Institute of Oncology, Bucharest, Romania

<sup>4)</sup>Department of Oral Rehabilitation, Faculty of Dentistry, "Titu Maiorescu" University, Bucharest, Romania

<sup>5)</sup>Department of Pathophysiology, "Iuliu Hațieganu" University of Medicine and Pharmacy, Cluj-Napoca, Romania

<sup>6)</sup>Department of Obstetrics and Gynecology II, "Iuliu Hațieganu" University of Medicine and Pharmacy, Cluj-Napoca, Romania

## Abstract

Breast cancer is a condition with the highest incidence of all neoplasms and a frequent cause of death. Due to increased incidence and mortality, this disease motivates healthcare professionals to redirect efforts to develop effective strategies for secondary prophylaxis. Imagistic investigations play an important role both in detecting lesions and in post-therapeutic evolutionary follow-up. The objective of the paper is to study cases of premalignant and malignant tumors, with a view to their imagistic identification confirmed in terms of histopathology, to highlight the accuracy of the imagistic examination as an important factor in the diagnosis and adaptation of an appropriate therapeutic attitude. The study was performed on a batch of 768 patients admitted to the Department of Surgery III, "Prof. Dr. Alexandru Trestioreanu" Institute of Oncology, Bucharest, Romania. The classical examined hypothesis is local examination, mammography, ultrasound, with its variations, and histopathological (HP) confirmation, either by thick-needle biopsy puncture and/or tumor excision. By correlating with HP examination of the imagistic representation of the lesion, we can show the importance or limitation of each imagistic investigation, but especially its usefulness in the choice of therapeutic behavior. Breast cancer screening using classical techniques currently requires implementation of modern techniques to diagnose this disease.

**Keywords:** breast cancer, diagnosis, mammography, elastography, 2D echography, imaging accuracy.

## Introduction

Breast cancer is a pathology with a very high frequency in Romania and has a major psychological impact on affected women. Mammary pathology generally constitutes a major public health problem due to increased prevalence at national and international levels (one out of six women develop breast cancer over a lifetime). It occupies the 2<sup>nd</sup> place as occurrence incidence and the 4<sup>th</sup> place as mortality rate, according to the latest *World Health Organization* (WHO) Reports [1–4].

The "gold standard" is the early and accurate detection of cancer or potentially neoplastic lesions, often silent but with major socioeconomic and psychological impact [5].

The research has been performed in patients who have had symptoms and those who discovered their lesions by routine screening [6].

In the recent years, studies have focused on the use of ultrasound (US), elastosonography, magnetic resonance imaging (MRI), other new morpho-imaging methods, and the translation of image characteristics by the Breast Imaging-Reporting and Data System (BI-RADS) Classification (*American College of Radiology*, 2003) for increasing sensitivity and specificity of breast cancer diagnostics [7].

The role of US has increased in recent years due to advances in diagnostic methods. High-resolution US detects small lesions and increases the accuracy of differentiation a benign and a malignant solid lesions. Another important element is tumor angiogenesis that can be investigated by using spectral Doppler, color or power Doppler [8, 9].

Mammography is the basic technique for detecting asymptomatic lesions, thus reducing mortality. To detect subtle and small size lesions, digital mammography superior to classical mammography was introduced regardless of the density or heterogeneity of the breast tissue [10].

Ultrasonography was developed for clinical trials, allowing for the reconstruction of tissue elasticity distribution, revealing the physical properties of tissues. The technique differentiates the hardness between pathological and normal tissues by calculating the axial hardness along the US direction. This method is complementary to two-dimensional (2D) US and thus increases the exam specification [11, 12].

Therefore, the main aim of our paper is to correlate the data obtained with new, modern imaging techniques that is confirmed histopathologically, in order to initiate a correct, adequate and individualized treatment for each patient.

## Patients, Materials and Methods

For our analysis, a BI-RADS  $\leq 2$  score was considered benign, a BI-RADS 3 score was considered as equivocal and a BI-RADS  $\geq 4$  score was considered malignant. Seven hundred sixty-eight patients were included in the study, divided into two groups, according to the BI-RADS score, as follows: Group I ( $n=358$ , BI-RADS  $\leq 3$ ) and Group II ( $n=410$ , BI-RADS  $\geq 4$ ).

The groups of patients that we studied were admitted in the Department of Surgery III, “Prof. Dr. Alexandru Trestioreanu” Institute of Oncology, Bucharest, Romania, between November 1, 2015–June 1, 2018.

Descriptive statistical elements were calculated, data presented using centrality, location and distribution indicators. For normal distribution testing, the Shapiro–Wilk test was used. In the case of non-uniform distribution values, the Mann–Whitney test ( $U$ ) was used. The significance threshold was  $\alpha=0.05$  (5%),  $\alpha=0.01$  (1%) or  $\alpha=0.001$  (0.1%).

To analyze the ability of some of the diagnostic methods to provide the correct diagnosis, the diagnostic test was used, the methods being related to the histopathological (HP) diagnosis, considered a certainty of diagnosis (“gold standard”). The diagnostic test was performed for the following types of investigations: mammography (M), mammography + ultrasound (M + US), and ultrasound + elastography (US + ES), taking into account: sensitivity (Sn) – positive test in a sick person; specificity (Sp) – negative test in a person without illness; accuracy (Acc) – ratio between the number of persons correctly diagnosed and total number of tested persons; positive predictive value (PPV); likelihood ratio (LR) – positive LR [ $LR+ = Sn / (1-Sp)$ ] and negative LR [ $LR- = (1-Sn) / Sp$ ]; diagnostic odds ratio (DOR) that combines Sn, Sp, PPV and negative predictive value (NPV) [ $DOR = (\text{true positive} / \text{false negative}) / (\text{false positive} / \text{true negative})$ ] in a single number.

The three diagnostic methods were also compared, in which case the positive concordance (pC) (equivalent to Sn), the negative concordance (nC) (equivalent to Sp), and the absolute concordance (aC) (equivalent to diagnosis Acc) were calculated.

The  $\chi^2$  (chi-square) test was also used to compare the different diagnostic methods. Relative risk or risk ratio (RR) was calculated as risk of exposed (RE) / risk of non-exposed (RN) ratio.

Statistical processing was performed with the StatsDirect v.2.7.2 and OpenEpi v.3.03 applications. The graphical representation of the results was done with the Excel application (from the Microsoft Office 2010 package).

The US images come from three ultrasounds, namely: Chison Q5, a portable color Doppler US with 7.5 MHz linear probe [year of manufacture (YoM) 2018, China]; Hitachi Aloka Arietta V70, equipped with power Doppler, elastography and linear probe up to 13 MHz (YoM 2017, Japan); Siemens Acuson S2000, equipped with linear probe up to 30 MHz, real-time sonoelastography, power Doppler (YoM 2017, Japan).

Tissue samples were obtained by tumors processing

into the Laboratory of Pathology, “Prof. Dr. Alexandru Trestioreanu” Institute of Oncology, Bucharest, according with Romanian Government Ordinance No. 1217/2010 (Annex 1) on indicative working techniques for the processing and staining of cytopathological and HP preparations (Figure 1).

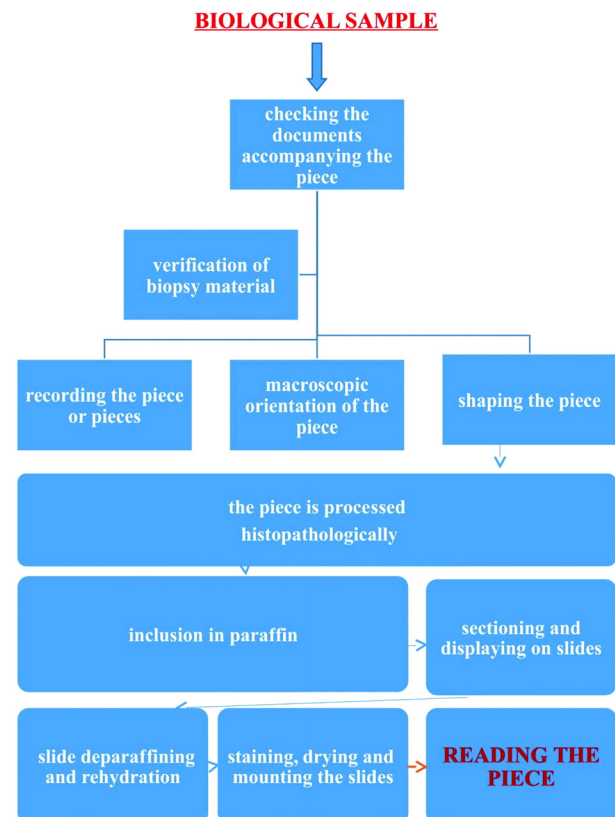


**Figure 1 – Working protocol for the biological piece (sample).**

The piece brought after orientation was fixed in 10% formalin for 24 hours and then processed in the FTP300 histology vacuum human tissue processor (Bio-Optica, Italy). After processing the fragments, they were introduced into the Microm EC 350 paraffin inclusion station (Thermo Scientific, Germany). The paraffin blocks were cut into 4–5 mm fragments on a Microm HM325 rotary microtome (Thermo Scientific, Germany). After cutting, the sections were laid on slides and stained on an Autocolor Touch 16-1600/T (Bio-Optica, Italy) device.

The staining was done with Hematoxylin–Eosin (HE). Manually mounted sections were sent to the pathological anatomy specialist, who read them using an AmScope B4908-314 microscope (Japan).

## Ethics

The study was conducted following a protocol approved by the Ethics Commission of the “Prof. Dr. Alexandru Trestioreanu” Institute of Oncology, Bucharest (Approval No. 15920/12.11.2018).

The study and working protocol were explained to the patients. Following the given consent, according to the Law on the protection of personal data, the study was carried out in accordance with the legislation in force.

## Results

A total number of 768 patients were studied and divided into two groups, according to the BI-RADS Classification (Table 1).

**Table 1 – The distribution of the patients by BI-RADS Classification**

BI-RADS Classification	No. of patients	Group
BI-RADS 1	68	I
BI-RADS 2	126	
BI-RADS 3	164	
BI-RADS 4	218	II
BI-RADS 5	192	

BI-RADS: Breast Imaging-Reporting and Data System.

As a representation of the age groups, the patient groups are divided as follows: for the age range of 30–40 years – 26 patients; 41–50 years – 72 patients; the highest number was in the range of 51–60 years – 386 patients; 61–70 years – 226 patients; over 70 years – 58 patients. The highest distribution was found for patients between 50 and 70 years old, accounting for 80% of all investigated cases, resulting in an increased incidence of malignant lesions in adult patients included in this age range.

The average age of the patients under study was 58.41 years ( $n=768$ , range 30–92 years). For patients in Group I, the average age was 54.41 years ( $n=358$ , range 32–83 years); they were divided into two subgroups, according to the HP examination results: subgroup  $I_B$ , with benign HP score and an average age of 54.55 years ( $n=349$ , range 32–83 years); subgroup  $I_M$ , with HP malignancy score and an average age of 48.89 years ( $n=9$ , range 34–66 years).

For patients in Group II, the average age was 61.91 years ( $n=410$ , range 30–92 years); they also were divided

into two subgroups, according to the HP examination results: subgroup  $II_B$ , with a benign HP outcome and an average age of 56.71 years ( $n=159$ , range 30–88 years); subgroup  $II_M$ , with a malignant HP result and an average age of 65.2 years ( $n=251$ , range 31–92 years) (Table 2).

**Table 2 – Age of the studied patients: average  $\pm$  SD [years] and statistical significance**

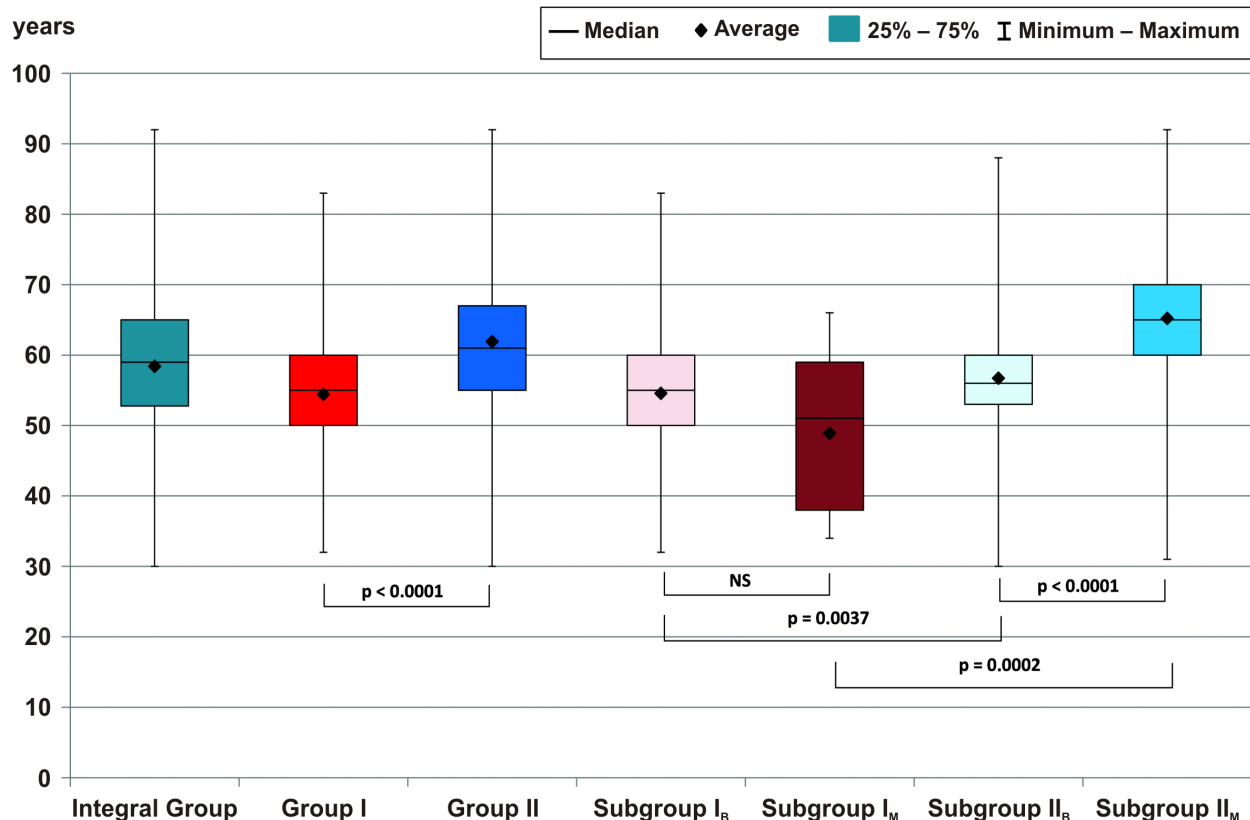
Group	Average $\pm$ SD	Statistical significance ( <i>p</i> )	
I	54.41 $\pm$ 8.69	I vs. II	<0.0001
II	61.91 $\pm$ 9.52		
I <sub>B</sub>	54.55 $\pm$ 8.56	I <sub>B</sub> vs. II <sub>B</sub>	0.0037
II <sub>B</sub>	56.71 $\pm$ 7.54	I <sub>M</sub> vs. II <sub>M</sub>	0.0002
I <sub>M</sub>	48.89 $\pm$ 12.14	I <sub>B</sub> vs. I <sub>M</sub>	0.1903
II <sub>M</sub>	65.2 $\pm$ 9.18	II <sub>B</sub> vs. II <sub>M</sub>	<0.0001

SD: Standard deviation.

During the statistical analysis of patient age values, statistically significant differences were observed between the patients' age by groups and subgroups, as follows:  $II > I$  ( $p < 0.001$ ),  $II_B > I_B$  ( $p < 0.01$ ),  $II_M > I_M$  ( $p < 0.001$ ), and  $II_M > II_B$  ( $p < 0.001$ ). The age difference between subgroups  $I_B$  and  $I_M$  was not statistically significant ( $p > 0.05$ ) (Figure 2).

The investigations done on the first group of patients (Figure 3) were increased in M (158 patients), M + 2D echography (2D Echo) (64 patients) followed by 2D US + ES (84 patients), on the opposite side being MRI-type investigations combined with M + US (24 patients).

For the second group of patients (Figure 4), complex-imaging investigations with M + 2D Echo predominated, the smallest number being recorded in MRI-combined 2D Echo. These differences are also due to the need of investigating and identifying the high-risk lesions and to improve a correct diagnosis.



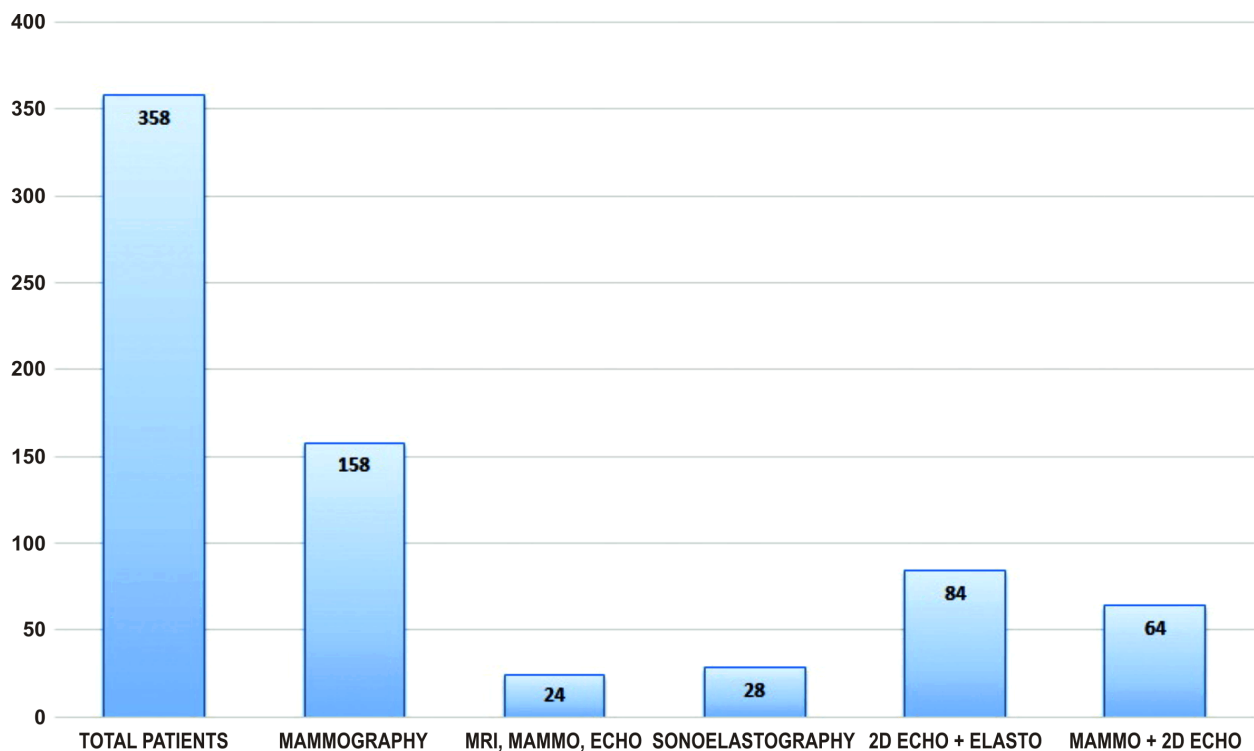


Figure 3 – The representation of the type of investigations done by Group I of patients. 2D: Two-dimensional; ECHO: Echography; ELASTO: Elastography; MAMMO: Mammography; MRI: Magnetic resonance imaging.

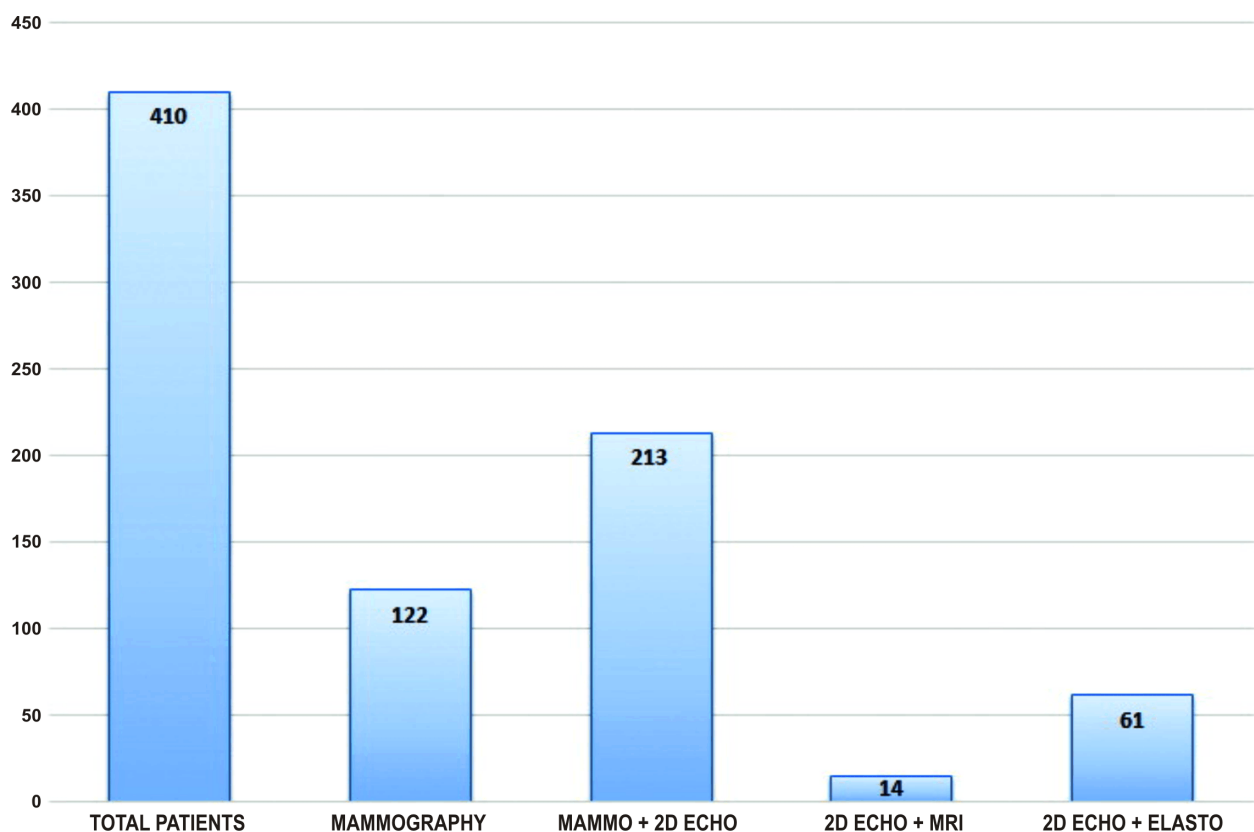


Figure 4 – The representation of the type of investigations done by Group II of patients. 2D: Two-dimensional; ECHO: Echography; ELASTO: Elastography; MAMMO: Mammography; MRI: Magnetic resonance imaging.

What we want to highlight in this study is the association of clinical symptomatology in conjunction with paraclinical and laboratory examinations, and the importance of each one only and them combined.

The common diagnostic methods used for both groups,

besides the HP examination, were M, M + US or US + ES. In these cases, for the evaluation of the diagnostic test, the HP examination (a diagnosis of certainty) was considered a “gold standard” (Table 3).

Thus, in the first group of 232 patients, 228 had benign

lesions and four patients had clinically and imagistically benign lesions but in terms of histopathology, they were confirmed to be malignant.

**Table 3 – Diagnostic imaging methods used**

Diagnostic method	Group I	Group II	Total
M	163	122	285
M + US	64	214	278
US + ES	83	61	144
US + M + MRI	24	0	24
US + MRI	0	14	14
ES	28	0	28

M: Mammography; US: Ultrasound; ES: Elastography; MRI: Magnetic resonance imaging.

Also, what we want to exemplify is that if the images shows us some typical lesion classifications and parameters, we do not have to forget to keep in touch even with the clinical aspects and the patient's symptomatology.

As we know, BI-RADS 1 to 3 show us benign lesions that need to be monitored, and maybe some BI-RADS 3 lesions need surgery. BI-RADS 4 and 5 lesions needs quickly surgery.

We will show some examples of cases of patients whose lesions were classified as benign but histopathologically confirmed to be malignant.

In Figure 5A is an US image of a patient presenting in the central area and especially retro-mammelonar a densification of breast tissue and ductal dilatations without pathological significance (BI-RADS 1 described), which requires follow-up over time. What disturbed the patient was the relatively abundant nipple secretion.

Figure 5B is the HP representation, which highlights an intraductal carcinoma described as tumor cell masses irregular in terms of shape and dimensions, with more prominent nuclei and nucleoli, with variable mitoses and perineural invasion.

Another specific case was that of a patient who has a hard-elastic formation, partially mobile on the deep planes, which presents the following imaging elements: hyper-echoic formation with slightly irregular contour, homogeneous content (BI-RADS 2) (Figure 6A). The HP correspondence of the lesion (Figure 6B) is a mucinous carcinoma that has as distinctive sign tumor cells "floating" in a large amount of mucin.

Figure 7A exemplifies the imaging aspect of a potentially benign lesion but which has two elements

raising questions: a bilobated solid, hypoechogenic solid formation with a clear contour, a slight posterior acoustic strengthening with the longitudinal axis parallel to the skin, small microcalcification area inside (BI-RADS 3).

According to the HP examination of the exeresis piece, it has been shown as being (Figure 7, B and C) on different sections a papillary carcinoma with tumor cells disposed in aggregates, which have round lumens in the center, tumor cells with intensely eosinophilic cytoplasm and round nuclei.

All the images below are representative cases of lesions that may or not be malignant. As we know, BI-RADS 4 classification tells us that the tumor is one that can be a malignant lesion, but sometimes some of the patients can have complex benign lesions that can look and feel like malignant tumors.

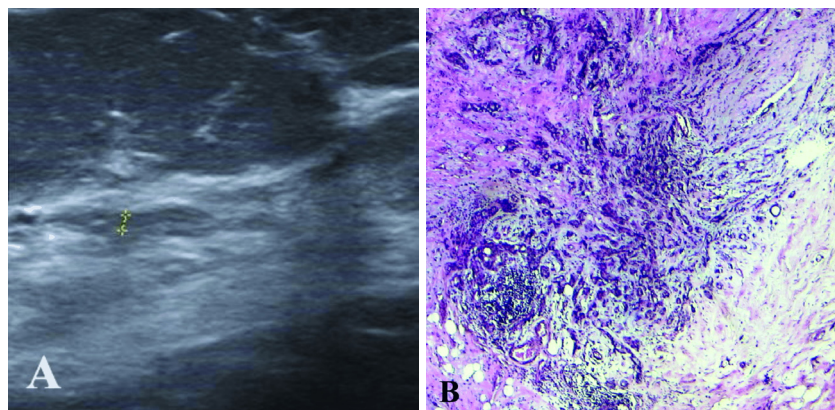
The images below (Figure 8, A and B) are the US translation of a potentially malignant lesion in clinical context (hard nodular formation, slightly irregular contour, semi-immobile to immobile on the lateral and deep planes, non-adherent to the tegument) and in terms of imaging (hypoechogenic polylobated formation with transonic images in the interior, with posterior acoustic strengthening, intensively vascularized – BI-RADS 4). Following these elements, it was decided to remove the lesion and was demonstrated in the HP result as a fibroadenoma with cystic microdilations.

In the image below (Figure 9A) is also exemplified a BI-RADS 4 type lesion but showing an elastographic intense and totally blue colored formation (Figure 9B) that represents a score 5, which is a potentially malignant lesion. Figure 9C is the HP representation of the lesion, which was found to be an invasive ductal carcinoma with placards, large cell nests with hyperchromic prominent nucleoli, which "float" in average amount of cytoplasm, accentuated nuclear pleomorphism, and microcalcification regions.

The last images represent the 2D US image and real-time sonoelastography of a potentially malignant breast lesion in a 43-year-old patient who, after the US, we completed her investigations with both M + breast MRI (Figure 10, A–D).

All imaging elements led to diagnosis of a BI-RADS 5 formation and elastographic score 5 and a strain hardness score of 75.33, with an E/2D improper ratio, which estimates a 100% malignant tumor.

**Figure 5 – (A) 2D echography: breast tissue with dilated ducts (BI-RADS 1); (B) Histopathological aspects of intraductal carcinoma lesion: tumor cell masses irregular in terms of shape and dimensions, with more prominent nuclei and nucleoli with variable mitoses (HE staining,  $\times 100$ ). 2D: Two-dimensional; BI-RADS: Breast Imaging-Reporting and Data System; HE: Hematoxylin–Eosin.**



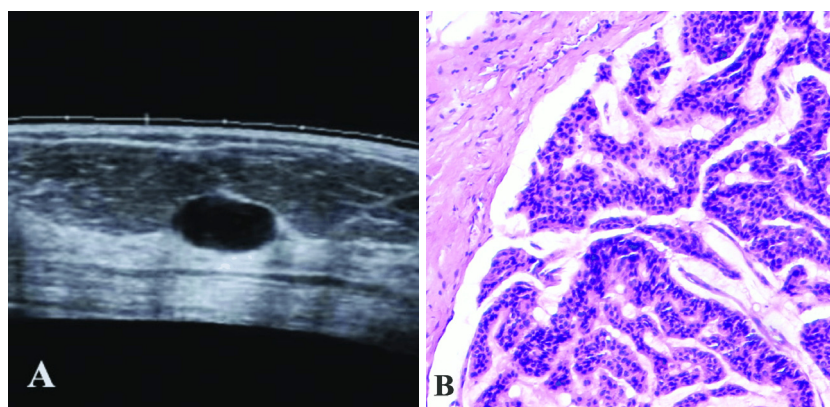


**Figure 6 – (A) 2D echography image of a hyperechoic formation with slightly irregular contour (BI-RADS 2); (B) Mucinous carcinoma: tumor cells “floating” in a large amount of mucin (HE staining,  $\times 200$ ). 2D: Two-dimensional; BI-RADS: Breast Imaging-Reporting and Data System; HE: Hematoxylin–Eosin.**

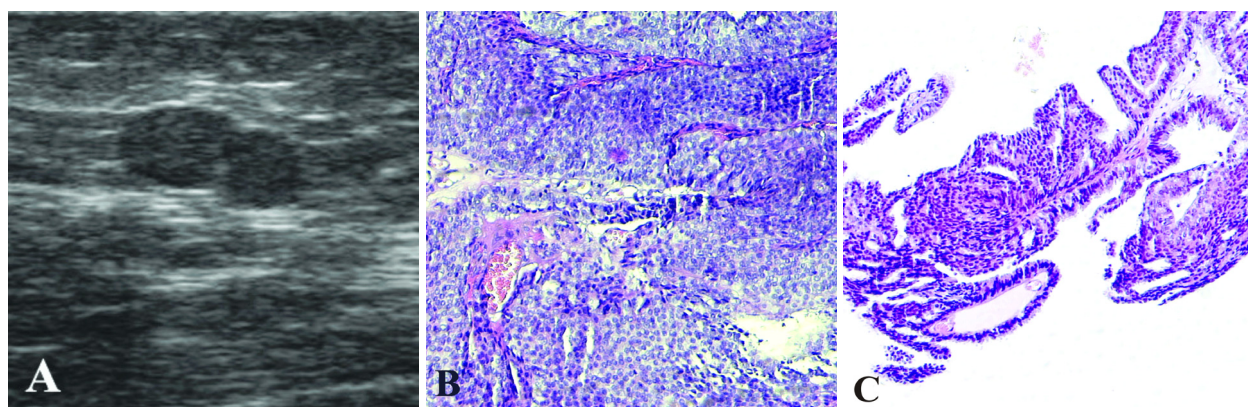


**Figure 7 – (A) 2D echography image of a bilobated lesion with calcification inside: posterior acoustic hardness; (B) Histopathological aspects of the lesion: papillary carcinoma; (C) Another section of the tumor: tumor cells disposed in aggregates, with round lumens in the center, intensely eosinophil cytoplasm and round nuclei. HE staining: (B)  $\times 100$ ; (C)  $\times 40$ . 2D: Two-dimensional; HE: Hematoxylin–Eosin.**

**Figure 8 – (A and B) 2D echography image of a fibroadenoma: hypoechoic polylobated formation with transonic images in the interior, with posterior acoustic strengthening, intensively vascularized (BI-RADS 4). 2D: Two-dimensional; BI-RADS: Breast Imaging-Reporting and Data System.**

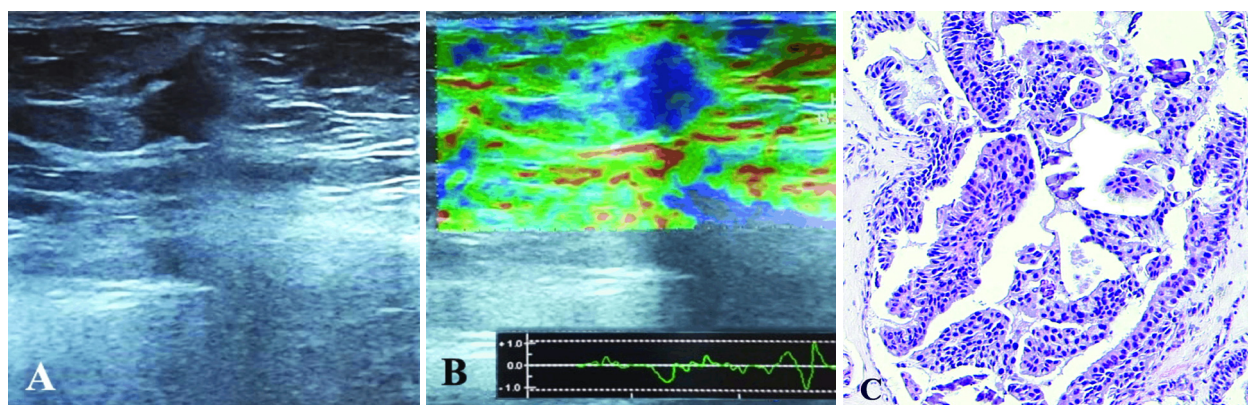
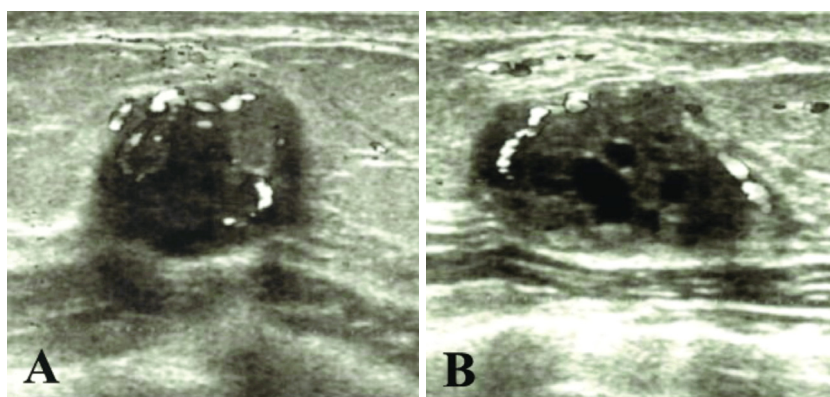


**Figure 9 – 2D echography (A) and elastosonography (B) of a hypoechoic formation, with a diffuse contour and vascularization – the intense blue color (elastographic score 5) of the tumor shows the hardness of the tumor mass (B); (C) Invasive ductal carcinoma with placards, large cell nests with hyperchromic prominent nucleoli, which “float” in average amount of cytoplasm, accentuated nuclear pleomorphism, and microcalcification regions (HE staining,  $\times 200$ ). 2D: Two-dimensional; HE: Hematoxylin–Eosin.**

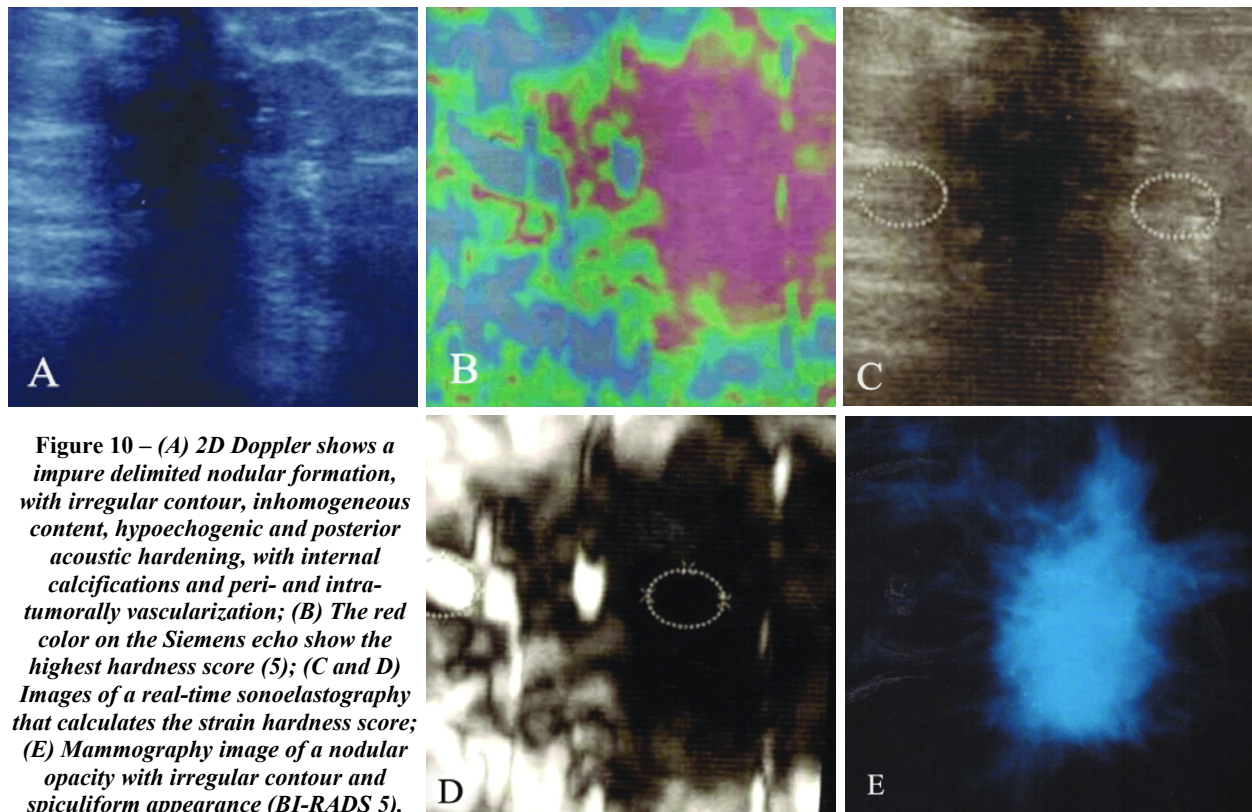


**Figure 10 – (A) 2D Doppler shows a impure delimited nodular formation, with irregular contour, inhomogeneous content, hypoechogenic and posterior acoustic hardening, with internal calcifications and peri- and intra-tumorally vascularization; (B) The red color on the Siemens echo show the highest hardness score (5); (C and D) Images of a real-time sonoelastography that calculates the strain hardness score; (E) Mammography image of a nodular opacity with irregular contour and spiculiform appearance (BI-RADS 5).**

**2D: Two-dimensional; BI-RADS: Breast Imaging-Reporting and Data System.**

When compared to HP, considered the “gold standard”, M + US Sn (99.26%) was higher than that of M (97.73%) and that of US + ES (88.46%). M diagnostic test had the highest Acc (86.67% vs. 71.52% and 71.22%, respectively).

LR was above all in all cases. DOR revealed that M had the most discriminatory power followed by the combination of M + US (Table 4).

**Table 4 – Diagnostic test indicators for M, M + US and US + ES as compared to the histopathological examination results**

Diagnosis methods	n	TP	FP	FN	TN	Sn	Sp	PPV	NPV	Acc	LR+	LR-	DOR
M	285	86	36	2	161	97.73	81.73	90.49	98.77	86.67	5.348	0.028	192.3
M + US	278	135	79	1	63	99.26	44.37	63.08	98.44	71.22	1.784	0.017	107.7
US + ES	144	23	38	3	80	88.46	67.8	37.7	96.39	71.53	2.747	0.17	16.14

M: Mammography; US: Ultrasound; ES: Elastography; n: No of cases; TP: True positive; FP: False positive; FN: False negative; TN: True negative; Sn: Sensitivity; Sp: Specificity; PPV: Positive predictive value; NPV: Negative predictive value; Acc: Accuracy; LR+/LR-: Positive/negative likelihood ratio; DOR: Diagnostic odds ratio.

The comparison of the three diagnostic tests, according to the HP results, showed for:

- M vs. M + US: aC 64.39%, pC 53.74%, nC 100%;
- M vs. US + ES: aC 57.64%, pC 0%, nC 100%;
- M + US vs. US + ES: aC 86.81%, pC 100%, nC 77.11%.

The *chi-square* test is a nonparametric concordance test used to test the significance of the association between two structures by comparing their frequencies.

In the comparative analysis between the three diagnostic imaging methods that were used in all patients, we observed:

- a statistically significant association between M and HP positive (malignant) diagnosis compared to US + ES ( $p=0.0065$ , RR 1.71, RE 30.88, RN 18.06);
- a statistically significant association between M + US and HP positive (malignant) diagnosis compared to M ( $p<0.0001$ , RR 1.584, RE 48.92, RN 30.88);

- a statistically significant association between M + US and HP positive (malignant) diagnosis compared to US + ES ( $p<0.0001$ , RR 2.709, RE 48.92, RN 18.06).

In the comparative analysis between the five diagnostic imaging methods that were used for Group I of patients, a statistically significant association between M and the HP negative (benign) diagnosis was observed compared to the M + US + MRI ( $p=0.0118$ , RR 1.129, RE 98.77, RN 87.5).

In the comparative analysis between the four diagnostic imaging methods that were used for Group II of patients, we observed:

- a statistically significant association between M and HP positive (malignant) diagnosis compared to US + ES ( $p<0.0001$ , RR 1.87, RE 70.49, RN 37.7);
- a statistically significant association between M + US and HP positive (malignant) diagnosis compared to US + ES ( $p=0.0007$ , RR 1.673, RE 63.08, RN 37.7).

## ✎ Discussions

National screening programs for preclinical breast cancer stages have been established in 18 countries [13].

Patients who were investigated by imaging methods had an oscillating distribution. An increased addressability was found for the group of patients aged 50–71, which represents about 80% of the whole group of women examined.

Most of the women were screened by M imaging. In the first group of women, most of them had M exams, 2D Echo and ES, and last but not least, M exams associated with 2D Echo. From the results, we can observe that M and M + US have a statistically significant association ( $p=0.0065$ , RR 1.71 and  $p<0.0001$ , RR 1.584, respectively).

The second group had more M associated with 2D Echo and less M single. The difference was because of the breast texture and largeness. This group had a statistically significant association M vs. M + US ( $p<0.0001$ , RR 1.87) and M + US vs. US + ES ( $p=0.0007$ , RR 1.673).

Romania is not part of the 18 countries that are performing active screening, but what we do is called opportunistic screening by taking care that we establish correct indications and parameters according to age, symptoms and risk factors [14].

By this study, we wanted to prove the correlation between the imaging and the HP examination and to highlight the accuracy rate of the imaging investigation diagnostic. We also want to relate the sensitivity and specificity of the investigations, thus proving the necessity of their use in medical practice and proving their usefulness and their indispensability in the case of small-infra-centimeter injuries and the early diagnosis of the cancer disease.

There have been cases in patients between 40–50 years old where we added mammary MRI with contrast agent for greater accuracy in setting the diagnosis. These patients were proven with BReast CAncer (BRCA) gene mutations and with historical family breast cancer cases. This proves that we apply the *European Society for Medical Oncology* (ESMO) Clinical Practice Guidelines and *American Society of Cytopathology* (ASC) Recommendations [15].

If some authors, such as Botticelli *et al.* [16–18], following a study on investigations of a group of patients, showed a diagnostic Acc score of 0.759, a Sn of 81% and a Sp of 75%, in our study we highlighted the following: a diagnosis Acc score of 0.678 of the cases examined, an average Sn of 95.15%, and an average Sp of 64.63%.

From the obtained values, we can assert that in the case of BI-RADS 4 lesions, the most appropriate is the association of imaging investigations and especially the use of “high class” investigations, such as real-time sonoelastography, sonography with contrast agent, mammography with tomosynthesis, and last but not least, MRI with contrast agent.

By developing radiology and combining investigations, we can get a Sp of 75–80% and a Sn of 93–98% in detecting occult or potentially malignant lesions, with a major impact in decreasing mortality and morbidity, but especially in choosing the right treatment. Early diagnosis also lowers the cost of breast cancer treatment so it can be strictly limited to the surgical side without the need for chemotherapy and/or radiotherapy.

The combination of imaging examinations greatly increases the diagnosis accuracy and the establishment of the appropriate therapeutic course.

In developed countries, such as the USA, the imaging investigations used, as Michael K. Pinkert [19–21] highlighted in the paper on quantified imaging, are microcomputed tomography (microCT), fluoroscopic US, very high frequency US, fluoroscopic molecular tomography, with a very high diagnosis accuracy, sensitivity and specificity. This suggests investing both in the preclinical, clinical and operational-medical field, which should also be the case for the country to invest in order to decrease mortality.

When we compared the imaging investigations to the HP results (considered the “gold standard”), the M + 2D Echo Sn (99.26%) was higher than that of M (97.73%) and that of 2D Echo + ES (88.46%). M diagnostic test had the highest Acc (86.67% vs. 71.52% and 71.22%, respectively). LR was above all in all cases.

At the end but not the least, breast cancer is an important factor of morbidity and mortality, with a very high incidence around the world, and especially in Romania, with a tendency of annual progressive increase, which has triggered a particular interest in the development of new imaging investigation techniques.

The results obtained in this study are encouraging and we believe that shortly the association of US with real-time sonoelastography will become routine investigations in senological practice, but we should not give up to mammograms.

## ✎ Conclusions

By correlating the imagistic methods with the examination of the HP piece, we can show the importance or limitation of each imagistic investigation, but especially its usefulness in the choice of therapeutic course. The development of radiology together with HP corroboration, and particularly biomarkers of predictive and progressive nature, can lead to the implementation of clinical strategy in choosing the appropriate therapeutic course, but especially in customizing and individualizing mammary tumors by cell types. At the end but not the least breast cancer is an important factor of morbidity and mortality, with a very high incidence around the world, and especially in Romania, with a tendency of annual progressive increase, which has triggered a particular interest in the development of new imaging investigation techniques.

## Conflict of interests

The authors declare that they have no conflict of interests.

## Funding sources

No funding was received for this work. This research did not receive any specific grant from funding agencies in the public, commercial, or not-for-profit sectors.

## References

- [1] Dowsett M, Dunbier AK. Emerging biomarkers and new understanding of traditional markers in personalized therapy for breast cancer. *Clin Cancer Res*, 2008, 14(24):8019–8026.
- [2] Siegel RL, Miller KD, Jemal A. Cancer statistics, 2017. *CA Cancer J Clin*, 2017, 67(1):7–30.

- [3] Ferlay J, Soerjomataram I, Ervik M, Dikshit R, Eser S, Mathers C, Rebelo M, Parkin DM, Forman D, Bray F. GLOBOCAN 2012 v1.0, cancer incidence and mortality worldwide: IARC Cancer Base No. 11. International Agency for Research on Cancer (IARC), Lyon, France, 2013, <http://globocan.iarc.fr>.
- [4] Bray F, Ren JS, Masuyer E, Ferlay J. Estimates of global cancer prevalence for 27 sites in the adult population in 2008. *Int J Cancer*, 2013, 132(5):1133–1145.
- [5] Ferlay J, Steliarova-Foucher E, Lortet-Tieulent J, Rosso S, Coebergh JWW, Comber H, Forman D, Bray F. Cancer incidence and mortality patterns in Europe: estimates for 40 countries in 2012. *Eur J Cancer*, 2013, 49(6):1374–1403.
- [6] Campeau PM, Foulkes WD, Tischkowitz MD. Hereditary breast cancer: new genetic developments, new therapeutic avenues. *Hum Genet*, 2008, 124(1):31–42.
- [7] \*\*\*. American College of Radiology (ACR) breast imaging reporting and data system (BI-RADS) atlas. ACR, Reston, VA, USA, 2003, [acr.org/birads](http://acr.org/birads).
- [8] \*\*\*. ACR Practice Guideline for the performance of ultrasound-guided percutaneous breast interventional procedures. ACR Resolution No. 29, revised 2009.
- [9] D'Orsi CJ, Sickles EA, Mendelson EB, Morris EA (eds). ACR BI-RADS® atlas: breast imaging reporting and data system. ACR, Reston, VA, USA, 2013.
- [10] Sippo DA, Warden GI, Andriole KP, Lacson R, Ikuta I, Birdwell RL, Khorasani R. Automated extraction of BI-RADS final assessment categories from radiology reports with natural language processing. *J Digit Imaging*, 2013, 26(5):989–994.
- [11] Taruttis A, van Dam GM, Ntziachristos V. Mesoscopic and macroscopic optoacoustic imaging of cancer. *Cancer Res*, 2015, 75(8):1548–1559.
- [12] Goddi A, Bonardi M, Alessi S. Breast elastography: a literature review. *J Ultrasound*, 2012, 15(3):192–198.
- [13] Giordano L, von Karsa L, Tomatis M, Majek O, de Wolf C, Lancucki L, Hofvind S, Nyström L, Segnan N, Ponti A; Eunice Working Group, Van Hal G, Martens P, Májek O, Danes J, von Euler-Chelpin M, Aasmaa A, Anttila A, Becker N, Péntek Z, Budai A, Mádaí S, Fitzpatrick P, Mooney T, Zappa M, Ventura L, Scharpantgen A, Hofvind S, Seroczynski P, Morais A, Rodrigues V, Bento MJ, Gomes de Carvalho J, Natal C, Prieto M, Sánchez-Contador Escudero C, Zubizarreta Alberti R, Fernández Llanes SB, Ascunce N, Ederra Sanza M, Sarriugarte Irigoien G, Salas Trejo D, Ibáñez Cabanell J, Wiege M, Ohlsson G, Törnberg S, Korzeniewska M, de Wolf C, Fracheboud J, Patnick JJ, Lancucki L, Ducarroz S, Suonio E. Mammographic screening programmes in Europe: organization, coverage and participation. *J Med Screen*, 2012, 19(Suppl 1):72–82.
- [14] Perry N, Broeders M, de Wolf C, Törnberg S, Holland R, von Karsa L. European Guidelines for Quality Assurance in breast cancer screening and diagnosis. Fourth edition – summary document. *Ann Oncol*, 2008, 19(4):614–622.
- [15] Warner E, Messersmith H, Causer P, Eisen A, Shumak R, Plewes D. Systematic review: using magnetic resonance imaging to screen women at high risk for breast cancer. *Ann Intern Med*, 2008, 148(9):671–679.
- [16] Botticelli A, Mazzotti E, Di Stefano D, Petrocelli V, Mazzuca F, La Torre M, Ciabatta FR, Giovagnoli RM, Marchetti P, Bonifacio A. Positive impact of elastography in breast cancer diagnosis: an institutional experience. *J Ultrasound*, 2015, 18(4):321–327.
- [17] Brunner AH, Sagmeister T, Kremer J, Riss P, Brustmann H. The accuracy of frozen section analysis in ultrasound-guided core needle biopsy of breast lesions. *BMC Cancer*, 2009, 9:341.
- [18] Landoni V, Francione V, Marzi S, Pasciuti K, Ferrante F, Saracca E, Pedrini M, Strigari L, Crecco M, Di Nallo A. Quantitative analysis of elastography images in the detection of breast cancer. *Eur Radiol*, 2012, 81(7):1527–1531.
- [19] Bae MS, Seo M, Kim KG, Park IA, Moon WK. Quantitative MRI morphology of invasive breast cancer: correlation with immunohistochemical biomarkers and subtypes. *Acta Radiol*, 2015, 56(3):269–275.
- [20] Garcia-Urbe A, Erpelding TN, Krumholz A, Ke H, Maslov K, Appleton C, Margenthaler JA, Wang LV. Dual-modality photoacoustic and ultrasound imaging system for noninvasive sentinel lymph node detection in patients with breast cancer. *Sci Rep*, 2015, 5:15748.
- [21] Jiang L, Greenwood TR, van Hove ER, Chughtai K, Raman V, Winnard PT Jr, Heeren RM, Artemov D, Glunde K. Combined MR, fluorescence and histology imaging strategy in a human breast tumor xenograft model. *NMR Biomed*, 2013, 26(3): 285–298.

### Corresponding author

Dan Nicolae Pătroi, Associate Professor, DMD, PhD, Department of Oral Rehabilitation, Faculty of Dentistry, “Titu Maiorescu” University, 67A Gheorghe Petrașcu Street, Sector 3, 031593 Bucharest, Romania; Phone +4021–325 14 16, e-mail: [dan.patroi@gmail.com](mailto:dan.patroi@gmail.com)

*Received: March 25, 2019*

*Accepted: January 30, 2020*